micromachines

MDPI

Article

Surface-Potential-Based Compact Modeling of p-GaN Gate HEMTs

Jie Wang [1], Zhanfei Chen [1,*], Shuzhen You [2], Benoit Bakeroot [3], Jun Liu [1] and Stefaan Decoutere [2]

1 The Key Laboratory for RF Circuit and Systems of Ministry of Education, Hangzhou Dianzi University, Hangzhou 310012, China; wangjie@hdu.edu.cn (J.W.); ljun77@hdu.edu.cn (J.L.)
2 Interuniversity Microelectronics Centre (IMEC), Kapeldreef 75, B-3001 Leuven, Belgium; shuzhen.you@imec.be (S.Y.); stefaan.decoutere@imec.be (S.D.)
3 CMST, IMEC, Ghent University, Technologiepark 126, B-9052 Ghent, Belgium; Benoit.Bakeroot@UGent.be
* Correspondence: chenzf@hdu.edu.cn

Abstract: We propose a surface potential (SP)-based compact model of p-GaN gate high electron mobility transistors (HEMTs) which solves the Poisson equation. The model includes all possible charges in the GaN channel layer, including the unintended Mg doping density caused by out-diffusion. The SP equation and its analytical approximate solution provide a high degree of accuracy for the SP calculation, from which the closed-form I–V equations are derived. The proposed model uses physical parameters only and is implemented in Verilog-A code.

Keywords: p-GaN gate high-electron mobility transistors; compact model; physics-based models; surface potential

check for updates

Citation: Wang, J.; Chen, Z.; You, S.; Bakeroot, B.; Liu, J.; Decoutere, S. Surface-Potential-Based Compact Modeling of p-GaN Gate HEMTs. *Micromachines* **2021**, *12*, 199. https://doi.org/10.3390/mi12020199

Academic Editor: Giovanni Verzellesi
Received: 20 January 2021
Accepted: 13 February 2021
Published: 15 February 2021

Publisher's Note: MDPI stays neutral with regard to jurisdictional claims in published maps and institutional affiliations.

Copyright: © 2021 by the authors. Licensee MDPI, Basel, Switzerland. This article is an open access article distributed under the terms and conditions of the Creative Commons Attribution (CC BY) license (https://creativecommons.org/licenses/by/4.0/).

1. Introduction

GaN based high electron mobility transistors (HEMTs), which are typically normally-on devices, draw significant attention for power switching applications due to the combined merits of a high OFF-state voltage and low ON-resistance R_{ON} originating from the high electron mobility and large breakdown electric field in these materials [1]. Yet the market demands for normally-off or enhancement mode (E-mode) devices. One of the approaches to obtain E-mode transistors is to use a p-GaN gate that lifts up the conduction band at the channel surface in equilibrium [2] and results in normally-off operation [3] by depleting the 2-D electron gas (2DEG) in the channel [4]. Today, the p-GaN gate devices were the first commercialized E-mode devices with high and robust threshold voltage V_{th}, high breakdown voltage, and low dynamic R_{ON} increase [5].

Effective circuit design using these devices requires fast and accurate models that can describe the behavior of the device under different working conditions. Previous work includes models such as the Curtice model [6], the Statz model [7], and the Angelov–Chalmers model [8], which are mostly empirical curve-fitting models that might not work well for large signal operation. DynaFET [9] is an innovative nonlinear model based on a non-linear network analyzer (NVNA) and an artificial neural network (ANN). These models hardly represent the physical GaN HEMT behavior, for they lack any predictive capability and are strictly limited to the test system. To overcome these difficulties, an exact, complete, and simple physics-based model is required. Two industrial standard models were recently selected by the CMC (Compact Model Council). First, there is the ASM model [10], a physics-based surface-potential (SP) model able to capture terminal characteristics of GaN HEMTs by solving the Schroedinger–Poisson coupled equations. Secondly, unlike SP-based models, the MIT Virtual Source GaN (MVSG) model [11] formulates mobile charge densities through a threshold voltage term. The physics-based MVSG model adopts a different interpretation of the carrier velocity by using an empirical saturation function for GaN HEMTs. Recently, a charge-based HEMT model was developed

by EPFL [12], starting from a physics-based model for regular silicon FETs and was given new physical quantities typical for HEMTs. However, the above models lack the physics of the typical gate structure in the p-GaN gate HEMTs, consisting of a "back-to-back" diode configuration [13].

Previously, we have developed a SP-based model for Schottky gate GaN HEMTs [14] which solved the problem of elaborate computations of the surface potential by using an approximate analytical solution. The goal of this work is to extend our model of the p-GaN HEMTs, by considering within the Poisson equation all possible charges induced: the polarization charges at the AlGaN/GaN and p-GaN/AlGaN interfaces, the active Mg doping in the AlGaN barrier and the GaN channel caused by out-diffusion [4], and holes. Our SP-based model is physics-based and precisely captures all operation regions in the Direct Current (DC) behavior. The model accuracy was demonstrated by the excellent agreement between the model and experimental data including Current–Voltage (I-V) and Capacitance–Voltage (C-V) results. The p-GaN gate HEMT model was implemented in Verilog-A, and the main characteristics of the device can be reproduced.

This brief is arranged as follows: In Section II, we present the device structure. Section III is divided in two subsections: (1) we describe the drain current (I_D) and gate current (I_G) models and (2) the gate, drain, and source charges are calculated. The model's implementation, parameter extraction, and experimental validation are discussed in Section IV. Finally, we conclude this paper.

2. Device Structure

The p-GaN gate HEMTs were fabricated in 200 mm pilot line using an Au-free process flow. Details of the process flow are described in [4]. Figure 1 shows a cross-section transmission electron microscope (TEM) picture of the gate area of a realized p-GaN gate HEMT. Table 1 is the main material properties in p-GaN gate HEMT.

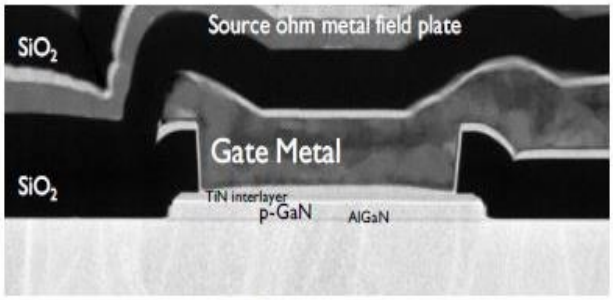

Figure 1. Transmission electron microscope(TEM) picture of the Schottky metal/p-GaN gate AlGaN/GaN high electron mobility transistors (HEMT).

Table 1. Main material properties in p-GaN gate HEMT.

Parameter	Physical Meaning	p-GaN HEMT
N_{Mg}	Mg density	3~5 × 10^{17} cm^{-3}
$E_{g\text{-}GaN}$	GaN Band gap	3.4 eV
ΔE_C	The Difference between the Conductor Bottom and Fermi Level	0.518 eV
N_C	GaN Conduction band density	2.02 × 10^{18} cm^{-3}
N_V	GaN Valence band density	9.08 × 10^{18} cm^{-3}
ε_{GaN}	GaN dielectric constant	9.4
ε_{AlGaN}	AlGaN dielectric constant	8.94

3. Surface Potential (SP)-Based Model

3.1. Current Calculation

First of all, it is important to concentrate on modeling the potential distribution along the channel of the p-GaN gate HEMTs. In order to obtain the electrostatic potential φ distribution in the p-GaN gate HEMTs, the 1D Poisson equation is solved in the GaN channel layer, in which the carrier density is determined by the polarization charges and the p-GaN gate at equilibrium [2]. Additionally, the p-GaN HEMTs feature unintended Mg doping density in the channel caused by out-diffusion, and thus the Poisson equation, including all possible charges within the device, must be considered. Since both the AlGaN and GaN layers are usually undoped, the depletion charge can be neglected. For completeness, we included hole charge density in the Poisson equation:

$$\frac{d^2\varphi}{dx^2} + \frac{d^2\varphi}{dy^2} = \frac{q}{\varepsilon_{GaN}}\left(N_{Mg} + n_{GaN} - p_{GaN}\right) \tag{1}$$

where ε_{GaN} is the permittivity of GaN, N_{Mg} is the unintended Mg doping in the channel caused by out-diffusion, φ is the surface potential, x is the direction along channel width, y is the direction perpendicular to the channel, n_{GaN} and p_{GaN} are the electrons' and holes' charge densities in the GaN channel layer, respectively.

The n_{GaN} and p_{GaN} are written as:

$$n_{GaN} = n_i \cdot \exp((-\Phi_F + \varphi - V_C)/V_T) \tag{2}$$

$$p_{GaN} = n_i \cdot \exp((\Phi_F - \varphi)/V_T) \tag{3}$$

The n_{GaN} and p_{GaN} can be represented in terms of the intrinsic carrier concentration n_i, the Fermi potential Φ_F ($\Phi_F = V_T[\ln(N/n_i)+2^{-1.5}(N/n_i)]$; N is the carrier concentration), the thermal voltage V_T ($V_T = kT/q$), and the voltage V_C applied between the channel and the substrate.

If we assume the gradual channel approximation that ignores the lateral field gradient in the Poisson equation, that is, ignore the y dependence of (x; y) in Equation (1), then we get:

$$\frac{d^2\varphi}{dx^2} = \frac{q}{\varepsilon_{GaN}}\left[n_i \exp\left(\frac{\varphi - \Phi_F - V_C}{V_T}\right) - n_i \exp\left(\frac{\Phi_F - \varphi}{V_T}\right) + N_{Mg}\right] \tag{4}$$

Defining a Gaussian surface from the GaN channel down to the neutral substrate gives the potential at x: $\varphi(x) = 0$ for $x \to \infty$ and $d\varphi(x)/dx = 0$ for $x \to \infty$. Imposing these boundary conditions gives, at $x = 0$, $\varphi(x = 0) = \varphi_{GaN}$ at the surface, where φ_{GaN} is the surface potential.

With the two-order integral from $\varphi = 0$ to $\varphi = \varphi_{GaN}$ of Equation (4), we can get the Surface-Potential Equation (SPE) shown in Equation (5), and this is the basis for our model.

$$V_G - V_0 - \varphi_{GaN} = \gamma\sqrt{\begin{array}{c}\frac{\varphi_{GaN}}{V_T}N_{Mg} + n_i \exp\left(\frac{-\Phi_F - V_C}{V_T}\right)\left[\exp\left(\frac{\varphi_{GaN}}{V_T}\right) - 1\right] \\ +n_i \exp\left(\frac{\Phi_F}{V_T}\right)\left[\exp\left(-\frac{\varphi_{GaN}}{V_T}\right) - 1\right]\end{array}} \tag{5}$$

In Equation (5), V_G is the gate voltage; γ is the body factor; V_0 is a fitting parameter such that the surface potential φ_{GaN} equals zero when $V_G = V_0$. We use an advanced non-iterative algorithm [15] to solve Equation (5) in a self-consistent way and obtain the potential distribution along the surface.

The surface potential φ_{pGaN} at the p-GaN/AlGaN layer interface is calculated with the same methodology [15].

$$\frac{d^2\varphi'}{dx^2} + \frac{d^2\varphi'}{dy^2} = \frac{q}{\varepsilon_{pGaN}}\left(N'_{Mg} + n_{pGaN} - p_{pGaN}\right) \tag{6}$$

where ε_{pGaN} is the permittivity of AlGaN; N'_{Mg} is the Mg doping in the p-GaN layer; n_{pGaN} and p_{pGaN} are the electrons' and holes' charge densities in the p-GaN layer, respectively.

The drain current is the most important device parameter of the HEMT device. The model uses drift-diffusion transport to calculate the drain current and adopts the channel current equation of the thin layer charge model [16] as:

$$I_D = -\mu W\left(q_i \frac{d\varphi_{GaN}}{dy} - V_T \frac{dq_i}{dy}\right) \tag{7}$$

where I_D is the drain current, q_i is the charge density in the GaN channel, μ is the electron mobility, and W is the gate width.

The p-GaN gate HEMTs, fabricated at IMEC, feature a TiN gate metal on top of the p-GaN layer in order to form a Schottky contact on the p-GaN to 2DEG gate input diode, to reduce the leakage current. Therefore, the gate leakage follows a path along this "back-to-back diode" structure [2].

According to the "back-to-back" diodes structure in the p-GaN gate HEMTs, the Schottky junction is reverse biased while the p-GaN/AlGaN/GaN junction is forward biased for higher gate voltages. The gate current can be calculated from the thermionic emission (TE) current over the AlGaN/GaN heterojunction with the current continuity condition [17]:

$$J_{TE} = \text{Area}\cdot J_{TE0} T^2 \left[\exp\left(\frac{\varphi_{pGaN} - \varphi_{GaN}}{n_{TE} V_T}\right) - 1\right] \tag{8}$$

where Area is the area of the gate, J_{TE0} is the current density of heterojunction which depends on the AlGaN/GaN barrier height, T is the temperature, and n_{TE} is the ideality factor for heterojunction.

At $V_G < 0$ V, the Schottky junction is forward biased, while the p-GaN/AlGaN/GaN junction is reverse biased, and the gate current is determined by a reverse leakage current along the edges of the gate and across the heterojunction. For this reverse leakage current, the hopping transport (HT) [18] model has been developed. The gate current empirically obeys the following equation:

$$J_{HT} = \text{Peri}\cdot J_{HT0}\left[\exp\left(\frac{\varphi_{pGaN}}{n_{HT} V_T}\right) - 1\right] \exp\left(-T^{-\alpha}\right) \tag{9}$$

where Peri is the perimeter of the gate, J_{HT0} is the reverse saturation current density, n_{HT} is the ideality factor, and α is the temperature coefficient [19].

3.2. Charge Calculation

The gate, drain, and source charges can be calculated by integrating the channel charge (q_{ch}) along the channel following the Ward–Dutton charge partitioning [20] as:

$$\begin{cases} Q_G = W\int_0^L q_{ch} dx \\ Q_D = W\int_0^L q_{ch}\frac{x}{L} dx \\ Q_S = W\int_0^L q_{ch}\left(1 - \frac{x}{L}\right) dx \end{cases} \tag{10}$$

where L is the channel length, W is the channel width and x is the position along the channel.

The integration in Equation (10) can be solved using the Symmetric Linearization Method [21] and neglecting the effect of velocity saturation on the charge.

The complete p-GaN gate HEMT structure contains several field plates (FPs), and therefore, attention is given to the accurate modeling of the FPs within the device. Given the field plate configuration depicted in Figure 2, the 2DEG is present below the FP at equilibrium. These field plate regions can be regarded as additional transistors in series with different threshold voltages. Hence, the field plate regions can be regarded as additional transistors in series with different operating voltages. The C–V behavior of a p-GaN gate HEMT is of utmost importance for the high-frequency performance and

switching characteristics of these high-power devices, and this is intrinsically related to the FP configuration. The equivalent circuit of capacitances is shown in Figure 2. The C–V characteristics can be modeled considering the capacitors with varying insulator thickness.

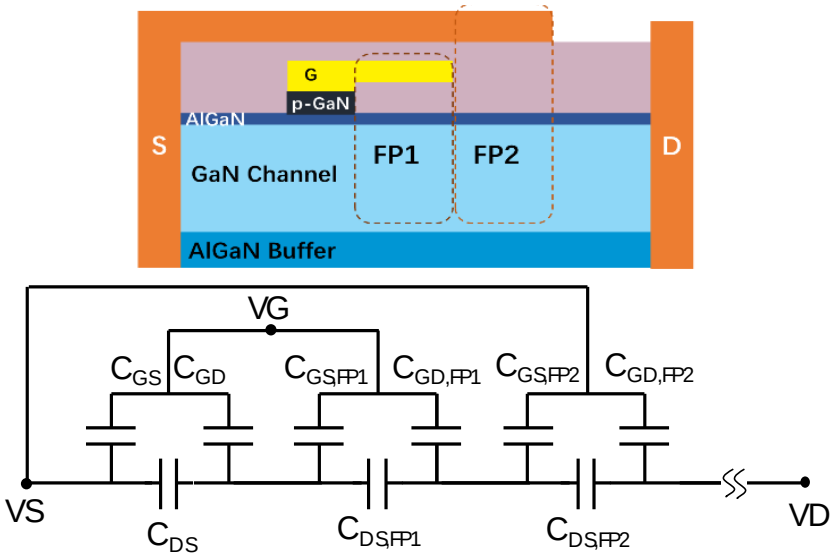

Figure 2. The equivalent circuit of the capacitance of field plates (FPs) of a p-GaN gate HEMT.

4. Results and Discussion

We have validated the proposed SP-based compact model using I–V and C–V measurement data of a typical 200 V p-GaN gate high-power HEMT device with a total device width W of 36 mm. The model is in good agreement with the measured currents, especially the gate current, and capacitances, as shown in Figures 3–7. For transconductance characteristics in Figure 3b, the effect of high electric field is lack in this model, which will be considered in the follow-up work to improve the accuracy.

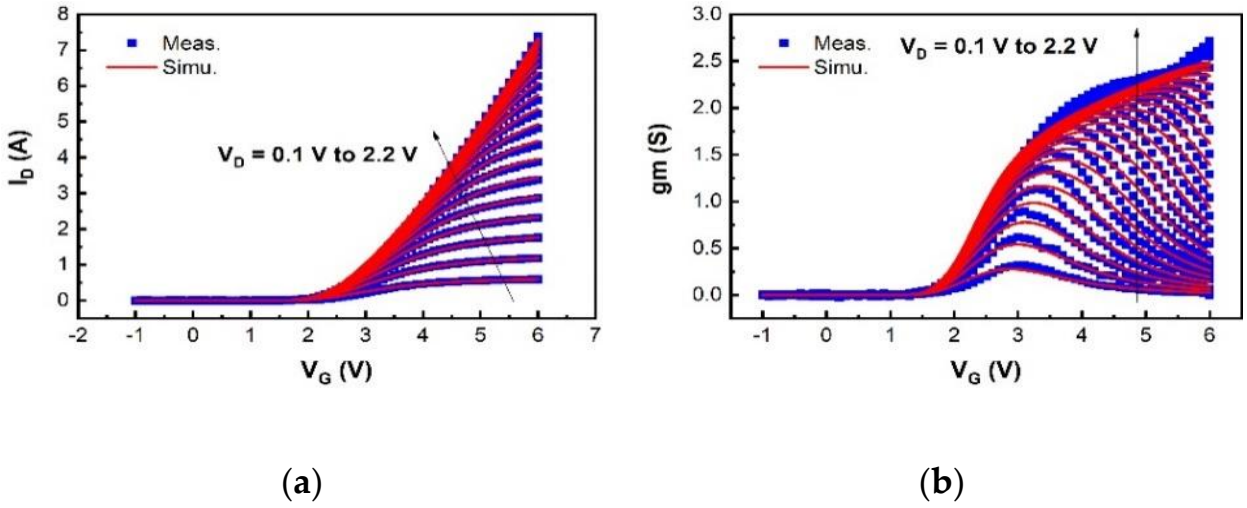

Figure 3. Measurement data (dots) and simulation data (line) at 300 K with V_D from 0.1 to 2.2 V, step = 0.1 V. (**a**) Transfer characteristics; (**b**) transconductance characteristics.

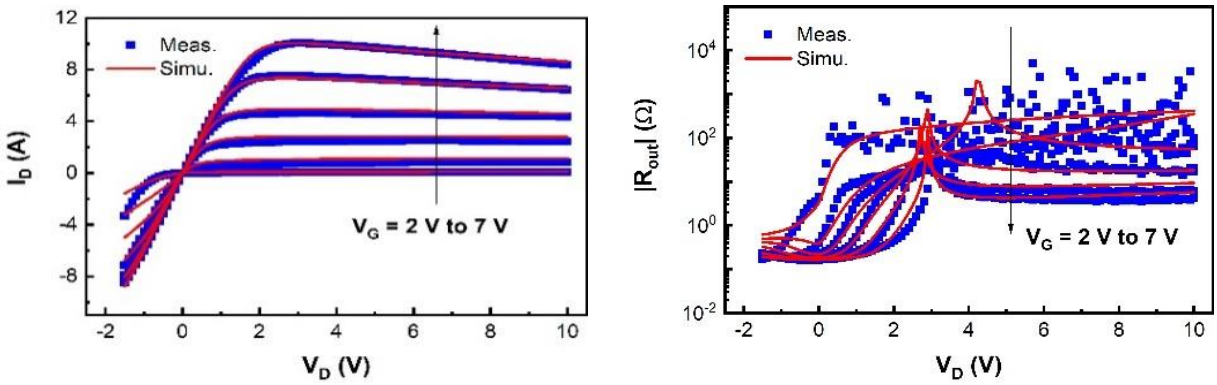

Figure 4. Measurement data (dots) and simulation data (line) at 300 K with V_G from 2 to 7 V, step = 1 V. (**a**) Output characteristics; (**b**) absolute values of output resistance characteristics.

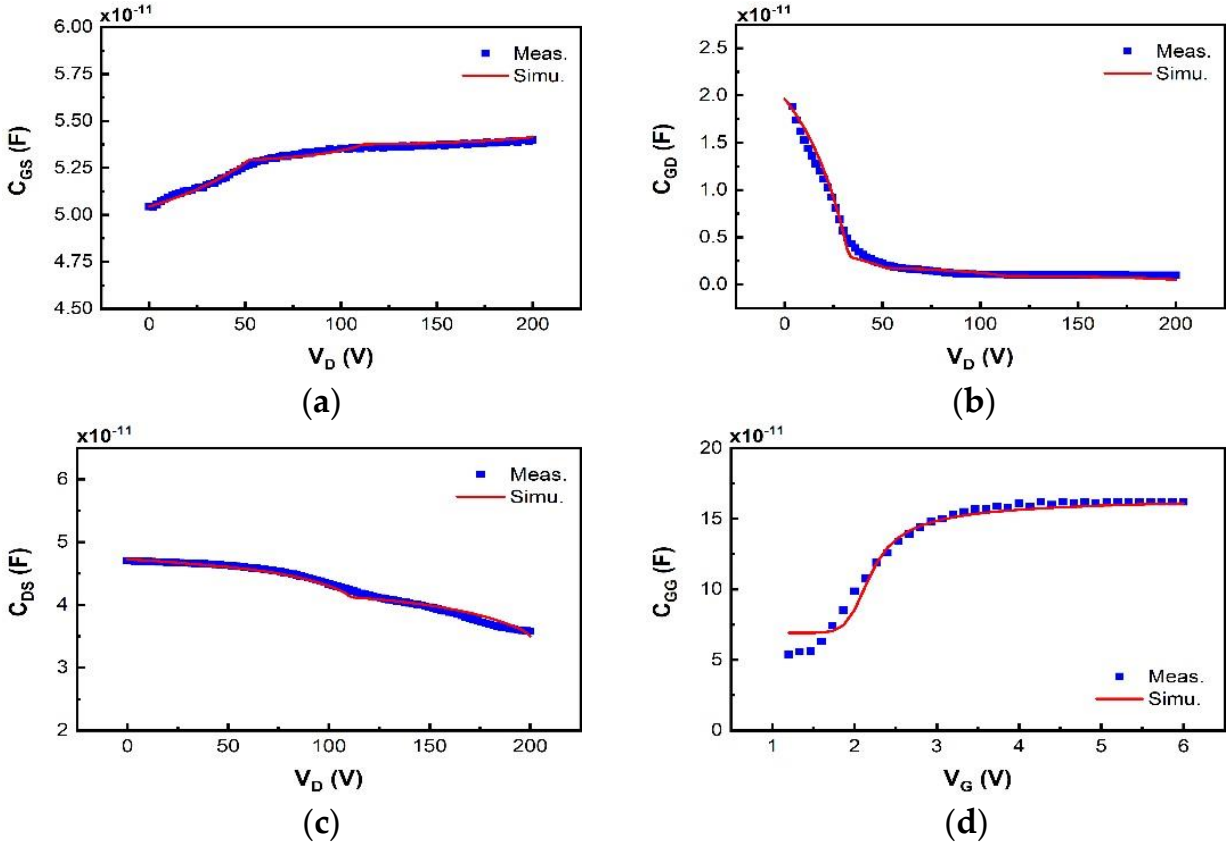

Figure 5. The C–V characteristics of the surface potential (SP) model (line) are compared with measurement data (dot) as a function of input voltage: (**a**) C_{DS} at different V_D; (**b**) C_{GD} at different V_D; (**c**) C_{GS} at different V_D; (**d**) C_{GG} (= C_{GS} + C_{GD}) at different V_G.

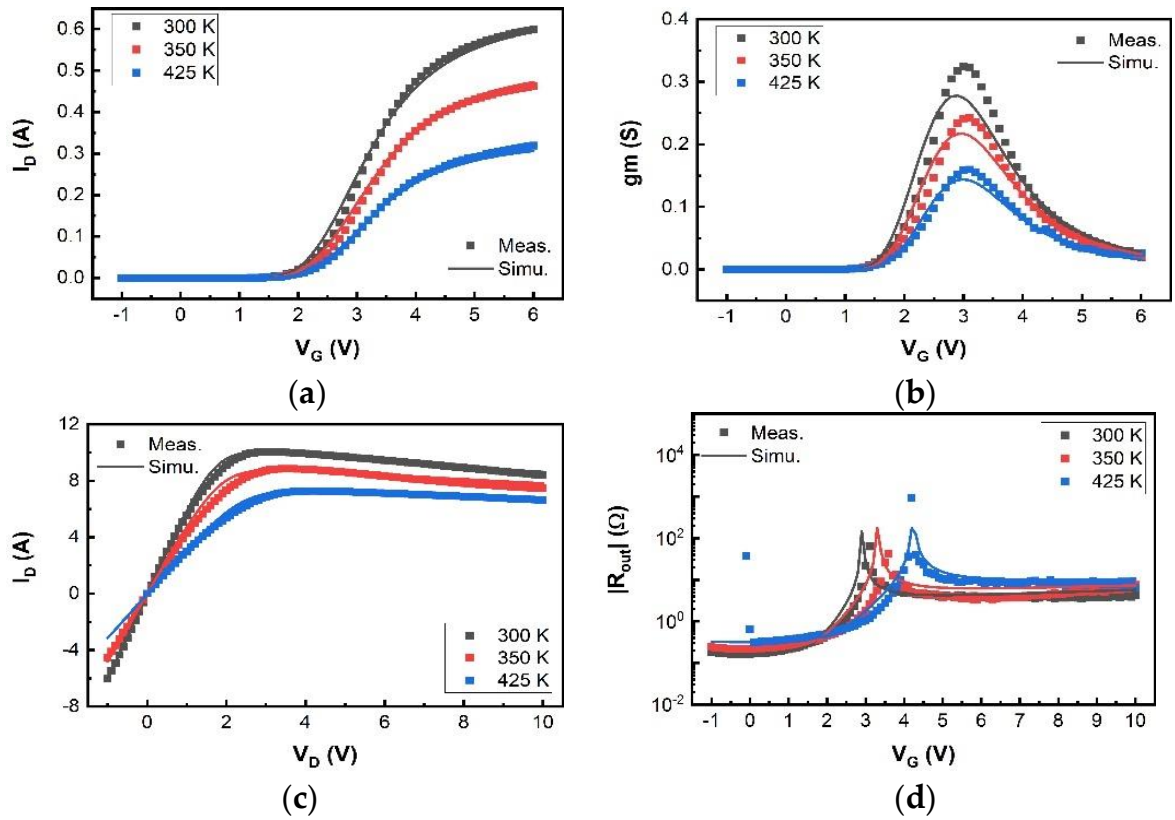

Figure 6. Measurement data (dots) and simulation data (line) at different temperatures. (**a**) Transfer characteristics with V_D = 0.1 V; (**b**) transconductance resistance characteristics with V_D = 0.1 V; (**c**) output characteristics with V_G = 7 V; (**d**) output resistance characteristics with V_G = 7 V.

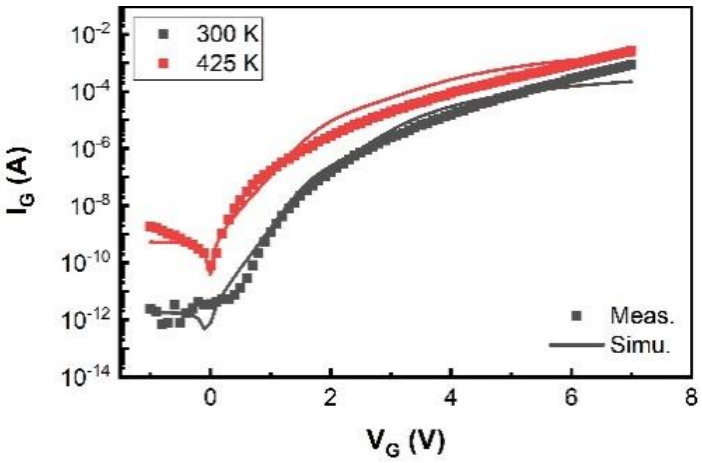

Figure 7. Measurement (dots) and simulation (lines) data of I_G at 300 and 425 K with V_{DS} = 0.1 V.

The simulated transfer and output characteristics match well with the measurement results at 300 K in Figures 3 and 4, sweeping V_G from −1 V to 6 V with V_D from 0.1 V to 2.2 V in I_D-V_G, and V_D from −1 V to 10 V with V_G from 2 V to 7 V in I_D-V_D. The OFF-state capacitances C_{GS}, C_{GD}, and C_{DS} at V_G = 0 V with V_D from 0 V to 200 V, are nicely modeled in Figure 5, capturing the impact of the field plates that modulate the 2DEG distribution at high V_D. The developed compact SP-based model successfully reproduces the measured current and capacitance characteristics.

The temperature dependence characteristics are also modelled and shown in Figure 6.

The Figure 7 shows an excellent agreement between the model and the measurement for both branches of $V_G \geq 0$ V and $V_G < 0$ V at different temperatures of 300 and 425 K.

5. Conclusions

The proposed SP-based compact model for p-GaN gate HEMTs is based on a surface-potential analytical approximate solution, which considers all possible induced charges at the AlGaN/GaN interface. This model gets the complete potential distribution along the surface by solving the Poisson equation. The developed compact model is physical as it includes the main GaN HEMT features in the solution of the Poisson equation. Good fit to the measurement results was obtained over a large range of gate and drain voltages. It was verified that this model can reproduce all observed current and capacitance characteristics of p-GaN gate HEMTs automatically.

Author Contributions: Writing—original draft preparation, J.W. and Z.C.; writing—review and editing, S.Y., B.B., J.L., and S.D. All authors have read and agreed to the published version of the manuscript.

Funding: This research was funded by the National Natural Science Foundation of China, grant number 61871161, and the Zhejiang Province Natural Science Foundation, grant number LZ17F010001.

Conflicts of Interest: The authors declare no conflict of interest.

References

1. Mishra, U.K.; Parikh, P.; Wu, Y.-F. AlGaN/GaN HEMTs-an overview of device operation and applications. *Proc. IEEE* **2020**, *90*, 1022–1031. [CrossRef]
2. Bakeroot, B.; Stockman, A.; Posthuma, N.; Stoffels, S.; Decoutere, S. Analytical Model for the Threshold Voltage of p-(Al)GaN High-Electron-Mobility Transistors. *IEEE Trans. Electron Devices* **2018**, *65*, 79–86. [CrossRef]
3. Marcon, D.; Saripalli, Y.N.; Decoutere, S. 200 mm GaN-on-Si epitaxy and e-mode device technology. In Proceedings of the 2015 IEEE International Electron Devices Meeting (IEDM), Washington, DC, USA, 7–9 December 2015.
4. Posthuma, N.E.; You, S.; Liang, H.; Ronchi, N.; Kang, X.; Wellekens, D.; Saripalli, Y.N.; Decoutere, S. Impact of Mg out-diffusion and activation on the p-GaN gate HEMT device performance. In Proceedings of the 28th International Symposium on Power Semiconductor Devices and ICs (ISPSD), Prague, Czech Republic, 12–16 June 2016.
5. Walter, R. Curtice. Nonlinear modeling of compound semiconductor HEMTs state of the art. In Proceedings of the IEEE MTT-S International Microwave Symposium Digest, Anaheim, CA, USA, 23–28 May 2010.
6. Chen, K.J.; Oliver, H.; Alex, L.; Chun, L.T.; Tetsuzo, U.; Yasuhiro, U.; Wu, Y.F. GaN-on-Si Power Technology: Devices and Applications. *IEEE Trans. Electron Devices* **2017**, *64*, 779–795. [CrossRef]
7. Statz, H.; Newma, P.; Smith, I.W. GaAs FET device and circuit simulation in SPICE. *IEEE Trans. Electron Devices* **1987**, *34*, 160–165. [CrossRef]
8. Angelov, I.; Zirath, H.; Rosman, N. A new empirical nonlinear model for HEMT and MESFET devices. *Microw. Theory Technol.* **1992**, *40*, 2258–2261. [CrossRef]
9. Xu, J.; Jones, R.; Harris, S.A.; Nielsen, T.; Root, D.E. Dynamic FET Model-DynaFET-for GaN Transistors from NVNA Active Source Injection Measurements. In Proceedings of the IEEE MTT-S International Microwave Symposium Digest, Tampa, FL, USA, 1–6 June 2014.
10. Ghosh, S.; Ahsan, S.A.; Dasgupta, A.; Khandelwal, S.; Chauhan, Y.S. GaN HEMT modeling for power and RF applications using ASM-HEMT. In Proceedings of the 2016 3rd International Conference on Emerging Electronics (ICEE), Mumbai, India, 27–30 December 2016.
11. Radhakrishna, U. Modeling Gallium-Nitride Based High Electron Mobility Transistors: Linking Device Physics to High Voltage and High Frequency Circuit Design. Ph.D. Thesis, Department of Electrical Engineering and Computer Science, Massachusetts Institute of Technology, Cambridge, MA, USA, 2016.
12. Jazaeri, F.; Sallese, J.M. Charge-Based EPFL HEMT Model. *IEEE Trans. Electron Devices* **2019**, *66*, 1218–1229. [CrossRef]
13. Stoffels, S.; Bakeroot, B.; Wu, T.L.; Marcon, D.; Posthuma, N.E.; Decoutere, S.; Tallarico, A.N.; Fiegna, C. Failure mode for p-GaN gates under forward gate stress with varying Mg concentration. In Proceedings of the IEEE International Reliability Physics Symposium (IRPS), Monterey, CA, USA, 2–6 April 2017.
14. Wang, J.; Sun, L.; Liu, J.; Zhou, M. A surface-potential-based model for AlGaN/AlN/GaN HEM. *J. Semicond.* **2013**, *34*, 0002–0007. [CrossRef]
15. Wang, J. Study on the Surface Potential-Based Model of GaN HEMT. Ph.D. Thesis, Department of Electrical Engineering, Zhejiang University, Hangzhou, China, 2013.
16. Brews, J.R. A Charge-Sheet Model of the MOSFET. *Solid -State Electron* **1978**, *21*, 345–355. [CrossRef]

17. Rhoderick, E.H.; Williams, R.H. Current-transport mechanisms. In *Metal-Semiconductor Contacts*, 2nd ed.; Clarendon: Oxford, UK, 1988; pp. 98–100.
18. Zhao, L.; Chen, L.; Yu, G.; Yan, D.; Yang, G.; Liu, B.; Gu, X.; Lu, H. Tunneling-Hopping Transport Model for Reverse Leakage Current in InGaN/GaN Blue Light-Emitting Diodes. *IEEE Photonics Technol. Lett.* **2017**, *29*, 1447–1450. [CrossRef]
19. Wang, J.; Chen, Z.; You, S.; Benoit, B.; Liu, J.; Sun, L.; Decoutere, S. Surface-Potential-Based Compact Model for the Gate Current of p-GaN Gate HEMTs. *IEEE Trans. Electron Devices* **2020**, *67*, 3564–3567. [CrossRef]
20. Oh, S.Y.; Ward, D.E.; Dutton, R.W. Transient analysis of mos transistors. *IEEE Trans. Electron Devices* **1980**, *27*, 1571–1578.
21. Gildenblat, G.; Li, X.; Wu, W.; Wang, H.; Jha, A.; van Langevelde, R.; Smit, G.D.J.; Scholten, A.J.; Klaassen, D.B.M. PSP: An Advanced Surface-Potential-Based MOSFET Model for Circuit Simulation. *IEEE Trans. Electron Devices* **2006**, *53*, 1979–1993. [CrossRef]